

**Supporting Information**

**Kinetics of Heterogeneous Reactions of Ozone with Representative PAHs and an Alkene at the Air–Ice Interface at 258 and 188 K**

Debajyoti Ray,<sup>1</sup> Hana Lišková,<sup>1</sup> Petr Klán\*,<sup>1,2</sup>

<sup>1</sup> Research Centre for Toxic Compounds in the Environment, Faculty of Science, Masaryk University, Kamenice 5, 62500 Brno, Czech Republic.

<sup>2</sup> Department of Chemistry, Faculty of Science, Masaryk University, Kamenice 5, 62500 Brno, Czech Republic.

**The Uptake Coefficient**

Adsorption of gaseous molecules is usually efficient due to the highly dynamic nature of the ice surface<sup>1</sup> but is not, in general, the rate determining step of a heterogeneous chemical reaction; thus the adsorption equilibrium is typically described by an air–ice partitioning coefficient  $K_{O_3}$ .<sup>2</sup>

**Table S1.** The partitioning coefficients obtained at 258 and 188 K<sup>a</sup>

	$K_{O_3}^{258\text{ K}} / \text{cm}^{-3}$	$K_{O_3}^{188\text{ K}} / \text{cm}^{-3}$
DPE <sup>b</sup>	$(1.5 \pm 0.04) \times 10^{-15}$	$(4.1 \pm 0.1) \times 10^{-8}$
STI	n.d. <sup>c</sup>	n.d. <sup>c</sup>
PER	$(9.2 \pm 0.6) \times 10^{-13}$	$(1.3 \pm 0.3) \times 10^{-11}$
ANT	$(3.3 \pm 0.1) \times 10^{-10}$	$(1.1 \pm 0.2) \times 10^{-9}$

<sup>a</sup> Calculated by fitting of the Langmuir–Hinshelwood equation to the data. <sup>b</sup> Determined in our previous study.<sup>3</sup> <sup>c</sup> Not determined; the  $K_{O_3}$  values could not be determined with confidence because reliable  $\ln(c_s/c_s^0)$  data could not be obtained at the highest  $[O_3]_g$ .

The apparent uptake coefficients,  $\gamma$ , which describes the probability that a gaseous molecule undergoing a kinetic collision with a surface is taken up (reacts),<sup>4</sup> were calculated according to the following equation:<sup>5,6</sup>

$$\gamma = \frac{4k_{\max}^1 K_{O_3}}{\sigma_S v_{O_3} (1 + K_{O_3} [O_3]_g)} \quad \text{Eq S1}$$

where  $\sigma_S$  is the substrate cross-section (estimated for DPE<sup>7</sup> and STI:  $6 \times 10^{-15} \text{ cm}^2 \text{ molecule}^{-1}$ , and ANT<sup>8</sup> and PER:  $8 \times 10^{-15} \text{ cm}^2 \text{ molecule}^{-1}$ );  $v_{O_3}$  is the ozone mean thermal velocity (here:  $2.88 \times 10^4 \text{ cm s}^{-1}$  at 188 K;  $3.37 \times 10^4 \text{ cm s}^{-1}$  at 258 K).  $\gamma$  decreases with increasing  $[O_3]_g$ ; the values of  $k_{\max}^1$ ,  $K_{O_3}$ , and  $[O_3]_g$  were calculated based on an approximation that the data obtained at 188 K can be explained by the Langmuir–Hinshelwood model (see the main text), and must be taken with caution.

## Lifetimes

The lifetime  $\tau$  of the studied compounds for a typical atmospheric ozone concentration in polar areas (50 ppbv) at both 258 and 188 K were estimated from the equation:<sup>9</sup>

$$\tau = ([O_3]^{1/2} + [O_3]_g) / k_{\max}^1 \cdot [O_3]_g \quad \text{Eq S2}$$

where  $[O_3] = 50 \text{ ppbv} \approx 1.2 \times 10^{12} \text{ molecules cm}^{-3}$ ,  $[O_3]^{1/2}$  is the ozone concentration when surface coverage is 0.5. The  $[O_3]^{1/2}$  values of STI, PER and ANT were estimated from the LH dependences: STI:  $2.0 \times 10^{14} \text{ molecules cm}^{-3}$ ; DPE:  $2.0 \times 10^{14} \text{ molecules cm}^{-3}$  (258 K),  $1.0 \times 10^{14} \text{ molecules cm}^{-3}$  (258 K); PER:  $4.0 \times 10^{15} \text{ molecules cm}^{-3}$  (258 K),  $4.5 \times 10^{15} \text{ molecules cm}^{-3}$  (188 K); ANT:  $3.0 \times 10^{15} \text{ molecules cm}^{-3}$  (258 K),  $3.5 \times 10^{15} \text{ molecules cm}^{-3}$  (188 K).

**Figures S1–S6.** Determination of the observed rate constants  $k_{\text{obs}}$  by plotting  $\ln(c_s/c_s^0)$  against reaction time using a weighted-least-squares method (where  $c_s^0$  is the initial substrate S concentration and  $c_s$  those obtained at the different reaction times). Ozone concentrations,  $[O_3]_g$ , and  $k_{\text{obs}}$  values are shown. Average values and error bars representing the standard deviation are given.

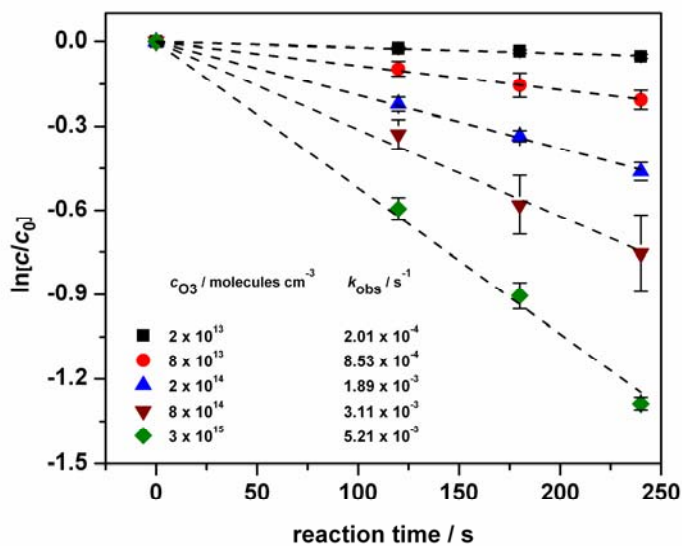


**Figure S1.** STI (258 K)

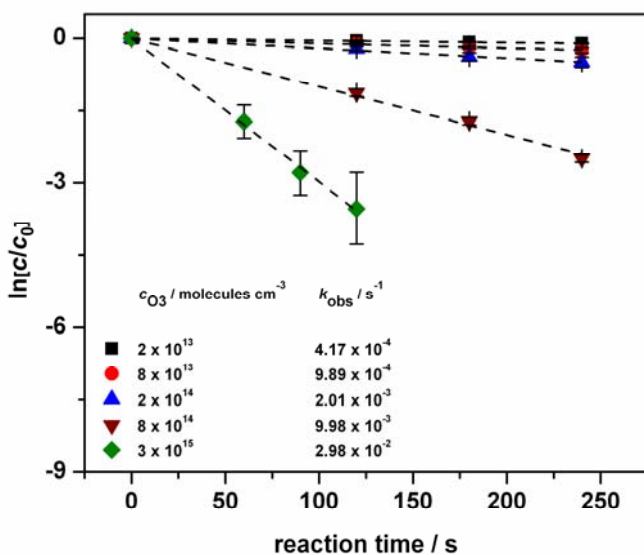


**Figure S2.** STI (188 K)

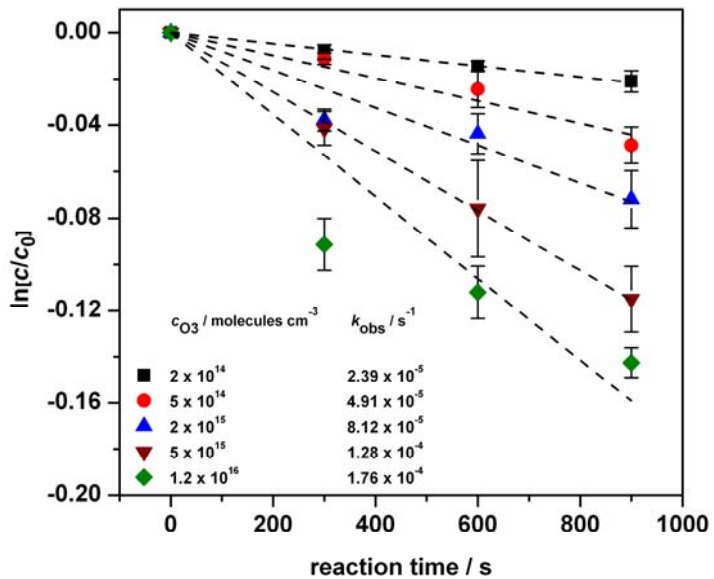


**Figure S3.** ANT (258 K)

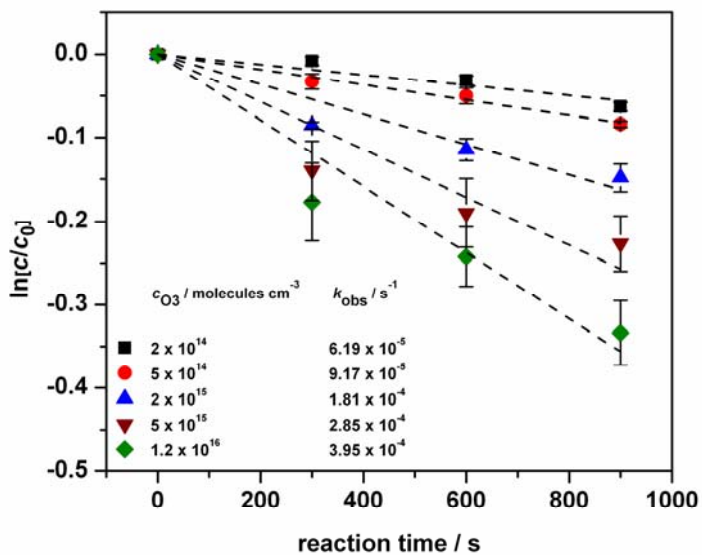


**Figure S4.** ANT (188 K)

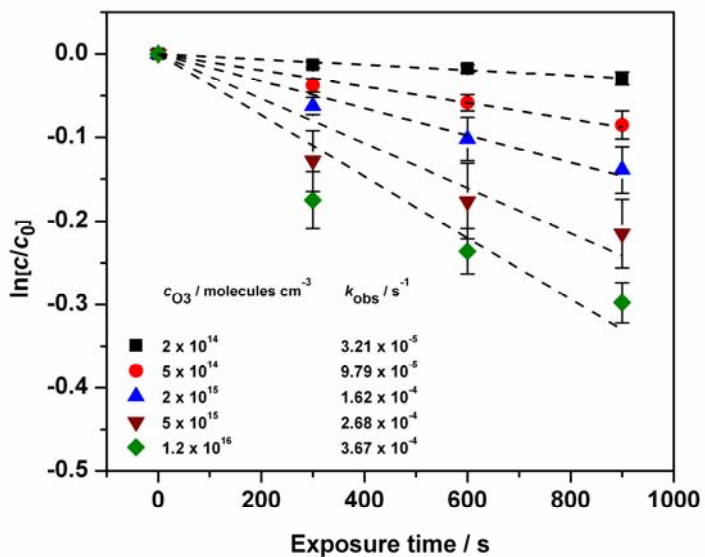


**Figure S5.** PER (258 K)

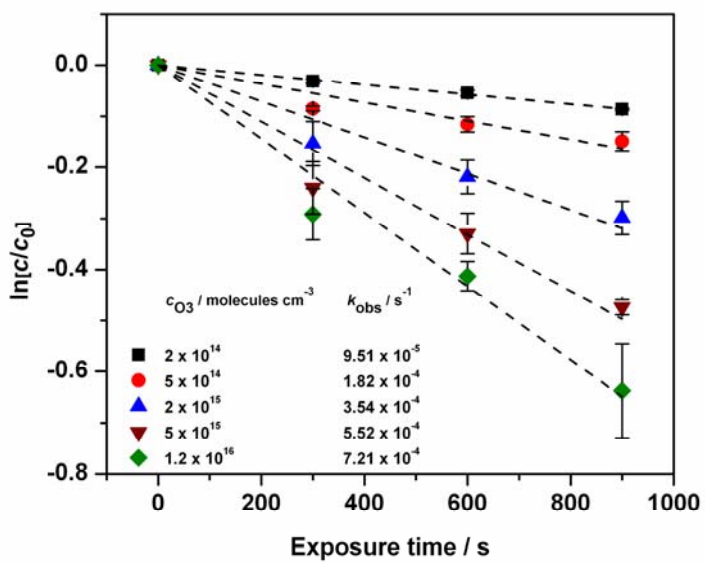


**Figure S6.** PER (188 K)

## References

1. J. P. D. Abbatt, *Chem. Rev.*, 2003, **103**, 4783-4800.
2. V. F. McNeill, A. M. Grannas, J. P. D. Abbatt, M. Ammann, P. Ariya, T. Bartels-Rausch, F. Domine, D. J. Donaldson, M. I. Guzman, D. Heger, T. F. Kahan, P. Klan, S. Masclin, C. Toubin and D. Voisin, *Atmos. Chem. Phys.*, 2012, **12**, 9653-9678.
3. D. Ray, J. K. E. Malongwe and P. Klán, *Environ. Sci. Technol.*, 2013, **47**, 6773-6780.
4. J. N. Crowley, M. Ammann, R. A. Cox, R. G. Hynes, M. E. Jenkin, A. Mellouki, M. J. Rossi, J. Troe and T. J. Wallington, *Atmos. Chem. Phys.*, 2010, **10**, 9059-9223.
5. U. Poschl, T. Letzel, C. Schauer and R. Niessner, *J. Phys. Chem. A*, 2001, **105**, 4029-4041.
6. M. Ammann, U. Pöschl and Y. Rudich, *Phys. Chem. Chem. Phys.*, 2003, **5**, 351-356.
7. D. Ray, R. Kurková, I. Hovorková and P. Klán, *Environ. Sci. Technol.*, 2011, **45**, 10061-10067.
8. J. Postma, S. Bari, R. Hoekstra, A. G. G. M. Tielens and T. Schlathoelter, *Astrophys. J.*, 2010, **708**, 435-444.
9. S. Raja and K. T. Valsaraj, *Atmos. Res.*, 2006, **81**, 277-292.